ELSEVIER

Journal of Power Sources 75 (1998) 13–18

JOURNAL OF POWER SOURCES

Discharge–charge characteristics and performance of Li/FeOOH(an) battery with PAN-based polymer electrolyte

K.S. Hwang *, T.H. Yoon, C.W. Lee, Y.S. Son, J.K. Hwang

Department of Chemistry, Pukyong National University, Pusan 608-737, South Korea

Received 24 February 1998; accepted 7 March 1998

Abstract

The discharge–charge characteristics and performance of a Li/FeOOH(an) solid polymer battery are investigated. The cell uses a cathode of amorphous FeOOH with aniline derivatives (FeOOH(an)) and a polyacrylonitrile-based solid polymer electrolyte. The ionic conductivity of the electrolyte sample used for electrochemical measurements is 1.6×10^{-3} Ω^{-1} cm^{-1} at room temperature. Its anodic stability is above 4.5 V. The diffusion coefficient of Li^+ ions into the cathode is found to be 2.97×10^{-11} cm^2 s^{-1} by a.c. impedance spectroscopy. Variations of impedance parameters and the diffusion coefficient are investigated during the first discharge–charge. From the results of these measurements, it is concluded that the structure of FeOOH(an) is deformed by Li^+ ion insertion/extraction. The electrochemical redox reaction of FeOOH(an) is investigated by cyclic voltammetry. In the potential range 2.0 to $\sim$4.0 V, the first discharge–charge is irreversible. Thereafter, reversible cycling processes take place. The initial discharge capacity is $\sim$130 mA h g^{-1} at a current density of 0.1 mA cm^{-2}.

Keywords: Lithium solid polymer battery; FeOOH(an); Diffusion coefficients; Impedance parameters

1. Introduction

The iron compound has been investigated as a cathode material for secondary lithium batteries because it has the advantages of cheapness and abundance. The compound FeOCl has been the subject of special interest by many researchers [1,2]. It is more reactive and is easily synthesized. On the other hand, its structure is not stable. Thus, it has been considered for primary lithium batteries. To overcome this limitation, workers [3–5] have examined the intercalation of organic compounds, such as Lewis bases, and have reported that modified FeOCl including aniline derivatives has improved specific energy and stability, as determined by the proportion of the aniline derivatives. FeOOH(an) was prepared and was used in secondary lithium polymer batteries. A solid polymer electrolyte (SPE) was used as the electrolyte. Generally, the SPE had only a low rate of self-discharge, good adhesion between the electrodes, and could be formed as a large-scale thin film. Polyacrylonitrile was used for the preparation of the solid polymer electrolyte. It has been reported [6] that PAN-based SPEs have high ionic conductivity and good mechanical properties.

In this work, a study is made of the basic characteristics and cycling performance of a Li/SPE/FeOOH(an) battery. The electrochemical behaviour is investigated by cyclic voltammetry. The diffusion coefficient of Li^+-ion insertion into the cathode is determined by a current–pulse relaxation method, chronoamperometry, and a.c. impedance spectroscopy [7]. The discharge–charge characteristics are also studied. In the first cycling process, various impedance parameters of the SPE/FeOOH(an) interface and the diffusion properties of Li^+ ions are investigated by a.c. impedance spectroscopy [8].

2. Experimental

2.1. Synthesis and identification of FeOOH(an)

The FeOCl was prepared by heating a α-Fe_2O_3 and anhydrous $FeCl_3$ mixture in 3:4 mole ratio in a sealed and evacuated Pyrex glass tube at 350°C for 3 days according to the method of Kanamura et al. [3]. The reaction product was washed with H_2O and acetone to remove excess

* Corresponding author. Tel.: +82-51-620 6371; fax: +82-51-628 8147; e-mail: kshwang@dolphin.pknu.ac.kr.

0378-7753/98/$19.00
PII S0378-7753(98)00077-9

$FeCl_3$, and then dried for 12 h at 80°C under vacuum. The FeOCl and aniline in a mole ratio of 4:1 were immersed in H_2O for 9 days at 30°C with stirring of the solution under an argon atmosphere. The products were washed with H_2O and acetone to remove any residual organic material adsorbed on the crystal surface. This was followed by drying for 12 h at 80°C under vacuum. The identification of aniline derivatives intercalated into FeOOH matrix was carried out by means of FT-IR spectroscopy (Spectrum 2000, Perkin Elmer, USA). The crystal structure was determined using a D/max-2000 X-ray diffractometer (Rigaku, Japan) with Cu K_α radiation.

2.2. Fabrication of composite cathode

The FeOOH(an) composite cathode was prepared by blending FeOOH(an) with polymer electrolyte and acetylene black at a wt.% composition of 35:10:55 by weight. The composition (wt.%) of solid polymer binder was 12 PAN:44 EC:44 PC:6 $LiClO_4$. The blended mixture was heated for 15 min at 110°C to obtain a slurry. The slurry was pasted on aluminium foil at a thickness of 100 to 150 μm, and then dried for 1 h at 60°C. Thereafter, it was pressed at 100 kg cm^{-2}.

2.3. Investigation of electrochemical behaviour

The redox reaction of FeOOH(an) in the discharge–charge process was investigated by cyclic voltammetry. The scan rate was 0.5 mV s^{-1}. The measurements were performed in potential range 1.5 to 4.5 V. Lithium electrodes were used as the reference and the counter electrodes. The FeOOH(an) composite cathode was used as the working electrode.

2.4. Determination of the diffusion coefficient of Li^+ ions into the cathode

The diffusion coefficient of Li^+ ions into the fresh cathode was determined by a current–pulse relaxation method, chronoamperometry, and a.c. impedance spectroscopy. For current–pulse relaxation, 1 mA was applied for 10 s and the transient open-circuit voltage was recorded. The chronoamperometric curve was obtained by stepping the electrode potential to 1.5 V vs. Li. The impedance spectrum was measured by applying an a.c. voltage of 10 mV amplitude over the frequency range 10^5 to 10^{-2} Hz. The geometric area of the composite cathode (1.33 cm^2) was used to determine the diffusion coefficient.

2.5. Fabrication of Li / FeOOH(an) battery

Li/FeOOH(an) solid-state polymer batteries were fabricated by sandwiching the polymer electrolyte laminate (100 to 150 μm) between a lithium foil anode ($\sim$ 50 μm) and a FeOOH(an) cathode ($\sim$ 150 μm). The sandwich was sealed in an aluminized polyethylene bag.

2.6. Investigation of the characteristics on the cycling process

The variation of potential was measured with respect to the insertion of LI^+ ions at the 1/10 C rate, and the interface impedance parameters of the SPE/FeOOH(an) cathode and diffusion properties were investigated at critical points during the first cycling process by means of a.c. impedance spectroscopy. The impedance spectra were measured after the electrode attained an equilibrium potential, namely, 5 min after interruption of the current. The capacity of the Li/FeOOH(an) polymer battery was investigated at various current densities, i.e., 0.1, 0.2, and 0.3 mA cm^{-2}. The cycleability was investigated at a current density of 0.2 mA cm^{-2}. These measurements were carried out with a battery cycling system (Arbin, USA).

3. Results and discussion

3.1. Characterization of FeOOH(an)

The FT-IR spectrum of FeOOH(an) is shown in Fig. 1. An absorption peak assigned to the stretching vibration of the O–H bond is observed at 3200 cm^{-1}. A broad adsorption peak is present at 500 cm^{-1}; this is associated with overtones of the lattice mode [5]. The absorption peaks assigned to the stretching vibration of the N–H bond appear at 3400 cm^{-1}. The absorption peaks in the range 700 to 1700 cm^{-1} correspond to the secondary phenylamines. This suggests that oligomers or polymers of phenylamines exist in the FeOOH(an) as aniline derivatives [5]. The crystal structure of the FeOOH(an) is amorphous. Lattice parameters for γ-FeOOH are observed in the XRD pattern. These results are consistent with those of Sakaebe and Higuchi [4] and Kanamura et al. [5].

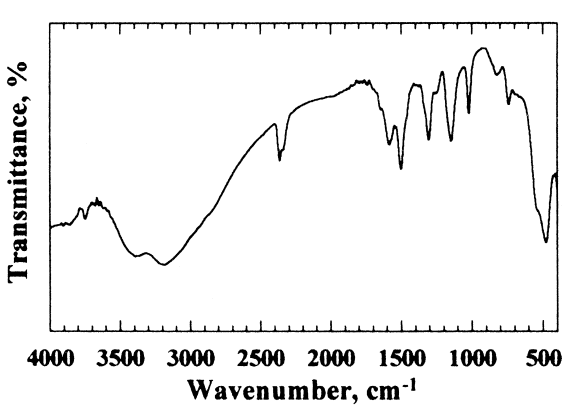

Fig. 1. FT-IR spectrum of FeOOH(an).

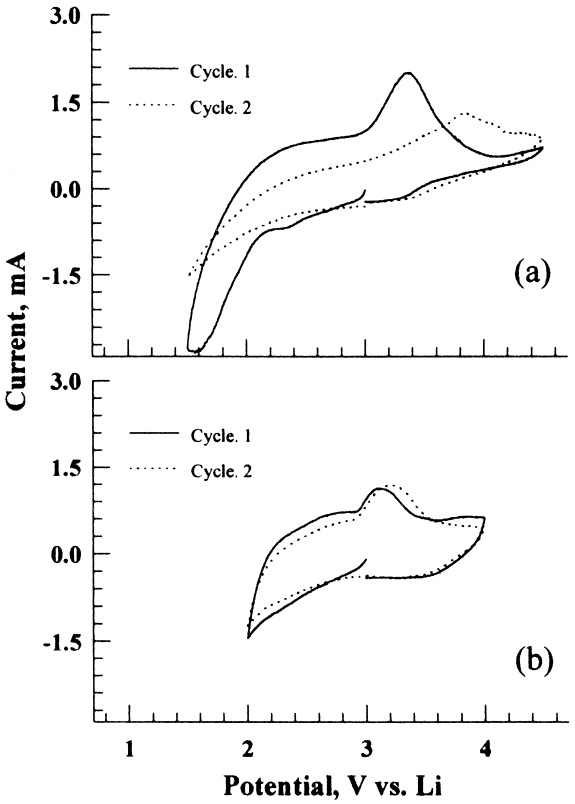

Fig. 2. Cyclic voltammograms for FeOOH(an). Potential range: (a) 4.5 to 1.5 V; (b) 4.0 to 2.0 V. Scan rate: 0.5 mV s^{-1}.

3.2. Characteristics of polymer electrolyte

The PAN-based polymer electrolyte was prepared according to the method of Abraham et al. [6]. The composition (mol.%) of the polymer electrolyte was 21 PAN:40.15 EC:32.85 PC:6 $LiClO_4$. The ionic conductivity was 1.6×10^{-3} Ω^{-1} cm^{-1} at room temperature. This indicates that application in a battery is feasible. The anodic stability was as high as 4.6 V. On the other hand, the interphase resistance of Li/SPE gradually increased with storage. This phenomenon is well known [9].

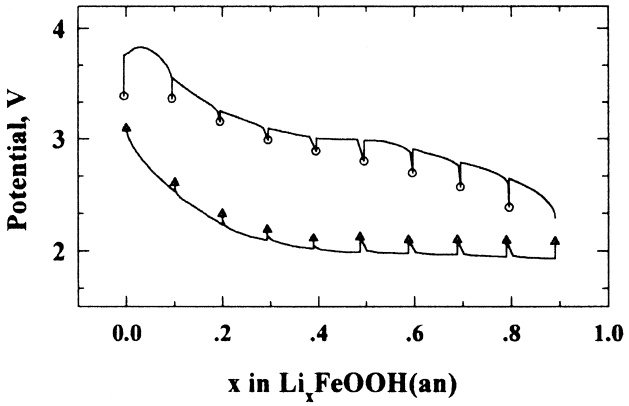

Fig. 4. Effect on potential of the lithium content intercalated in the composite cathode during initial discharge–charge process. Rate of discharge–charge = 1/10 C.

3.3. Electrochemical behaviour of FeOOH(an) cathode

Cyclic voltammograms for the FeOOH(an) cathode over different potential ranges are given in Fig. 2. Over the potential range 1.5 to 4.5 V (Fig. 2a), considerable changes occur in both the cathodic and anodic peaks on the second cycle and coulombic integral decreases to 50% of the initial cycle. These changes were also observed over the potential range 1.5 to 4.0 V, but not over 2.0 to 4.0 V. This suggests that the potential range of the first cathodic scan affects the behaviour of the second cycle. Thus, the deformation of the composite cathode is caused by excessive insertion of Li^+ ions into the FeOOH(an) cathode during the first cathodic scan.

3.4. Diffusion coefficient

The Nyquist plot of the SPE/FeOOH(an) cathode exhibits a semicircle at high frequencies, attributed to the charge-transfer process, and a linear portion with a phase angle of 45° attributed to the diffusion of Li^+ ions inside the cathode. The plot of Z_{re} against $\omega^{-1/2}$ (Randles' plot) is linear with a slope that corresponds to the Warburg

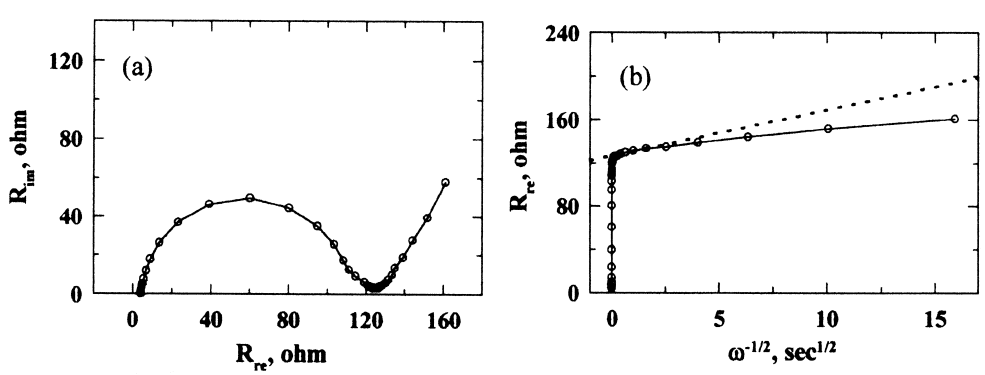

Fig. 3. Typical (a) Nyquist and (b) Randles plots of the interface of the SPE/fresh FeOOH(an) composite electrode.

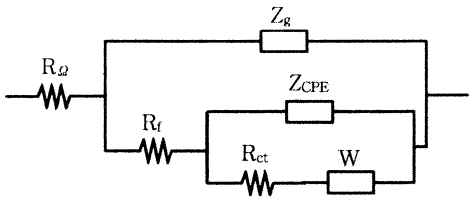

Fig. 5. Equivalent circuit of SPE/FeOOH(an) interface.

coefficient, σ, which is related to the diffusion coefficient, D, as follows [10]:

$$\sigma = \frac{RT}{n^2F^2A\sqrt{2}}\left(\frac{1}{D^{1/2}C^*}\right) \quad (1)$$

The Nyquist plot and Randles' plot of a fresh FeOOH(an) cathode are shown in Fig. 3. The Warburg coefficient is 8.46 $\Omega/s^{1/2}$ from which the diffusion coefficient is calculated as 2.97×10^{-11} cm^2 s^{-1}. The value of the diffusion coefficient determined by the current–pulse relaxation method and chronoamperometry was 1.4×10^{-8} and 1.1×10^{-8} cm^2 s^{-1}, respectively. These latter values are higher than that obtained from a.c. impedance spectroscopy. The current–pulse relaxation method and chronoamperometry techniques induce large changes in the local concentrations or in the states of charge. Thus, d.c. transient measurements were made after the d.c. polarization experiments for diffusion coefficient. By contrast, with the a.c. impedance method, the perturbation was restricted to a maximum of 10 mV. Thus, such changes were not induced. It is reasonable that higher values are obtained from d.c. transient measurements [6]. These values of the diffusion coefficient are similar to those of transition metal oxides. This indicates that normal diffusion of Li^+ ions is occurring inside the cathode.

3.5. Mechanism of redox reaction

The electrochemical behaviour of FeOOH(an) should depend on the aniline derivatives (PA) and the FeOOH matrix. Two processes are possible, namely:

$$PA^{x+}\left(ClO_4^-\right)_x + ye^- \leftrightarrow PA^{(x-y)+}\left(ClO_4^-\right)_{x-y} \quad (2)$$

$$FeOOH + xe^- + xLi^+ \leftrightarrow Li_xFeOOH \quad (3)$$

Kanamura et al. [5] have reported that the redox reaction of aniline derivatives in the FeOOH(an) is not involved in the anion doping and undoping processes. Therefore, the redox reaction of aniline derivatives should be coupled with the redox reaction of the FeOOH matrix [5]. The redox reaction of FeOOH(an) can be expressed as follows:

$$FeOOH(an) + xe^- + xLi^+ \leftrightarrow Li_xFeOOH(an) \quad (4)$$

Thus, Fe^{3+} ion is reduced to Fe^{2+} ion during discharge and Fe^{2+} is oxidized to Fe^{3+} during charge, in concert with lithium insertion and extraction, respectively. In these reaction processes, the relationship between the FeOOH matrix and the aniline derivatives is not known exactly.

The initial process of discharge–charge at the 1/10 C rate is shown in Fig. 4. During discharge, a plateau appears near 2.0 V at which the content of Li^+ ions inserted in the FeOOH(an) is 0.4. Although a plateau of 3.0 V is observed during charge, it is not reversible. The process of discharge–charge becomes reversible after the second cycle.

3.6. Interfacial properties on initial cycle

The variation in the impedance parameters with the insertion/extraction of Li^+ ions was investigated during initial discharge–charge at the 1/10 C rate. For these investigations, the equivalent circuit shown in Fig. 5 was

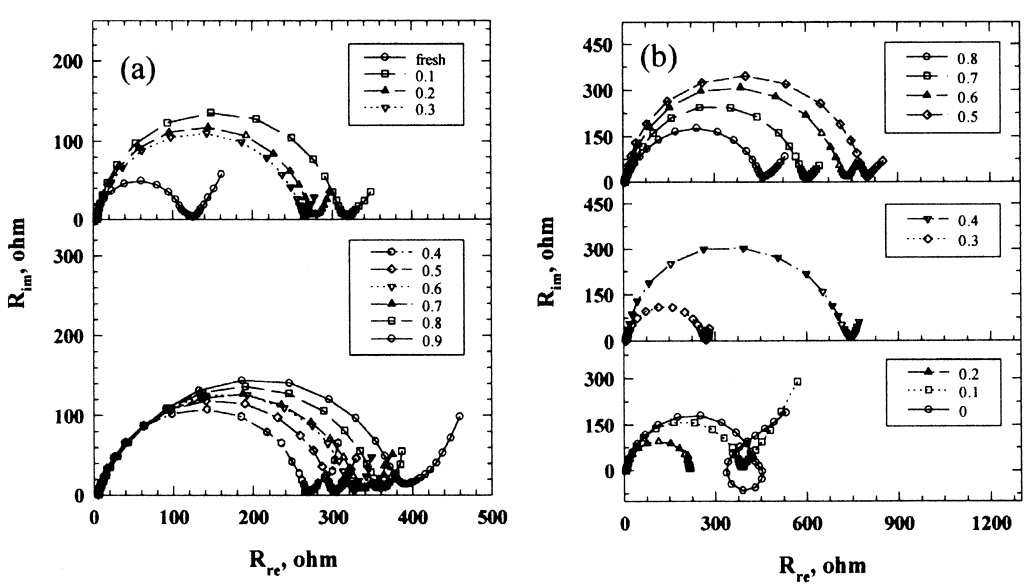

Fig. 6. Nyquist plots obtained from a three-electrode battery with lithium as a reference electrode for cathode/electrolyte interface during the initial (a) discharge and (b) charge. The composition of x in $Li_xFeOOH(an)$ is indicated.

assumed for the interface of the SPE/FeOOH(an) composite cathode. In this circuit, R_f is the film resistance of ClO_4^- oxidized on the cathode surface [11], R_{ct} is the charge-transfer resistance, Z_{CPE} is the impedance of the constant-phase element and is defined as [8]:

$$Z_{CEP} = A(j\omega)^{-\alpha}, \qquad j = \sqrt{-1} \tag{5}$$

where: ω is the angular frequency ($\omega = 2\pi f$); A is a constant which is related to R_{ct}; α is equal to $1-2\theta/\pi$. If α is 1, then θ is zero and Z_{CPE} becomes an ideal capacitor. α is a measure of the inhomogeneity of the interface.

Nyquist plots obtained from the impedance response are given in Fig. 6. These responses were obtained at various stages of discharge–charge at the 1/10 C rate. The impedance parameters are listed in Tables 1 and 2. R_{ct} is considerably increased during the initial discharge. This may be due to the coulombic attraction between the Li^+ ion and the oxide lattice. R_{ct} tends to decrease in range $x = 0.1$ to 0.4. This suggests that the coulombic attraction decreases during the process of discharge. On the other hand, R_{ct} increases again in range $x = 0.5$ to 0.9 and this is associated with a decrease in the diffusion coefficient of the Li^+ ion. The value of diffusion coefficient is maximum in the range $x = 0.5$ to 0.6, and then decreases for $x > 0.7$. Thus, the increase in R_{ct} over the range $x = 0.7$ to 0.9 is related to the decrease of the diffusion coefficient in the plateau region. Z_{CPE} continuously increases during the process of discharge. This indicates that charges accumulate continuously in the double layer of the SPE/FeOOH(an) cathode. The value of θ increases until $x = 0.5$, thereafter, it has a constant value. Thus, although the insertion of Li^+ ions affects the inhomogenity of the FeOOH(an) cathode, it becomes a constant phase in the plateau region. In other words, there is a change in the structure of the FeOOH(an) cathode during discharge. These structural changes have been investigated by XRD [5]. The variation in the impedance parameters during charge differs significantly from that during discharge. R_{ct} increases considerably over the range $x = 0.9$ to 0.5, but decreases suddenly in the range $x = 0.4$ to 0.3. This shows that the coulombic attraction between the Li^+ ion and the oxide lattice is increased compared with that during initial discharge. Moreover, the pattern of charge-transfer changes in the range $x = 0.4$ to 0.3. Thus, the coulombic attraction may be minimized by the positive charge of oxidized aniline derivatives. The θ and Z_{CPE} decrease until $x = 0.5$. This indicates that a less inhomogeneous FeOOH(an) cathode is formed due to the extraction of Li^+ ions and the positive charge of the aniline derivatives. These values at the termination of charge ($x = 0.2 \sim 0$) increase due to inhomogenity caused by the dissolution of Fe^{2+} ions. It is known [12] that the complicated Nyquist plot of $x = 0$ is induced by such dissolution. This dissolution also brings about a decrease in the diffusion coefficient.

Table 1
Impedance parameters and diffusion coefficients during initial discharge

x in Li_xFeOOH (an)	R_Ω (Ω)	R_f (Ω)	R_{ct} (Ω)	Z_{CPE} (μF)	θ (degree)	$D\times10^{11}$ ($cm^2\ s^{-1}$)
Fresh	4.24	–	107.98	8.14	4.6	2.97
0.1	5.13	–	301.67	7.82	5.5	3.22
0.2	4.89	–	268.18	10.15	7.5	4.50
0.3	5.23	–	256.68	11.82	9.0	4.65
0.4	5.06	–	260.44	13.05	10.6	4.85
0.5	5.18	–	293.78	13.13	12.6	8.65
0.6	5.42	–	313.91	14.70	11.8	9.00
0.7	5.46	–	319.35	16.13	13.4	3.98
0.8	5.59	–	342.73	16.56	12.2	4.88
0.9	5.84	–	363.41	16.15	12.7	2.32

Table 2
Impedance parameters and diffusion coefficients during initial charge

x in Li_xFeOOH (an)	R_Ω (Ω)	R_f (Ω)	R_{ct} (Ω)	Z_{CPE} (μF)	θ (degree)	$D\times10^{11}$ ($cm^2\ s^{-1}$)
0.8	5.93	17.20	432.57	19.06	11.8	1.47
0.7	5.69	11.64	576.57	15.31	9.2	3.63
0.6	5.82	5.07	706.02	13.84	7.7	4.17
0.5	5.89	2.25	781.57	11.62	6.4	3.17
0.4	6.44	–	717.39	13.77	7.9	2.67
0.3	7.28	–	254.54	13.98	8.0	3.24
0.2	5.47	–	214.48	12.25	7.0	
0.1	5.83	–	378.57	12.95	10.0	0.67
0	5.97	–	430.73	18.68	11.4	0.39

3.7. Cyclic performance

The relationship between the capacity and the current density is shown in Fig. 7. The initial discharge capacity at 0.1 mA cm^{-2} (about 1/14 C) is 130 mA h g^{-1} ($x = 0.6$) in the potential range 2.0 to 4.0 V. It is assumed that the molecular weight of FeOOH(an) is 120. The capacity decreases on increasing the current density. A specific plateau near 3.8 V appears on the termination of charge at 0.1 mA cm^{-2} and 0.2 mA cm^{-2}. This may be attributed to the oxidation of aniline derivatives and the dissolution of Fe^{2+} ion due to the extraction of most inserted Li^+ ions. The plateau is not observed after the second cycle.

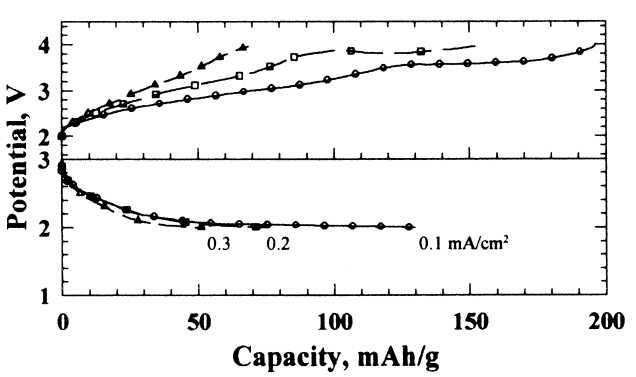

Fig. 7. Initial discharge and charge capacities at different discharge–charge current densities.

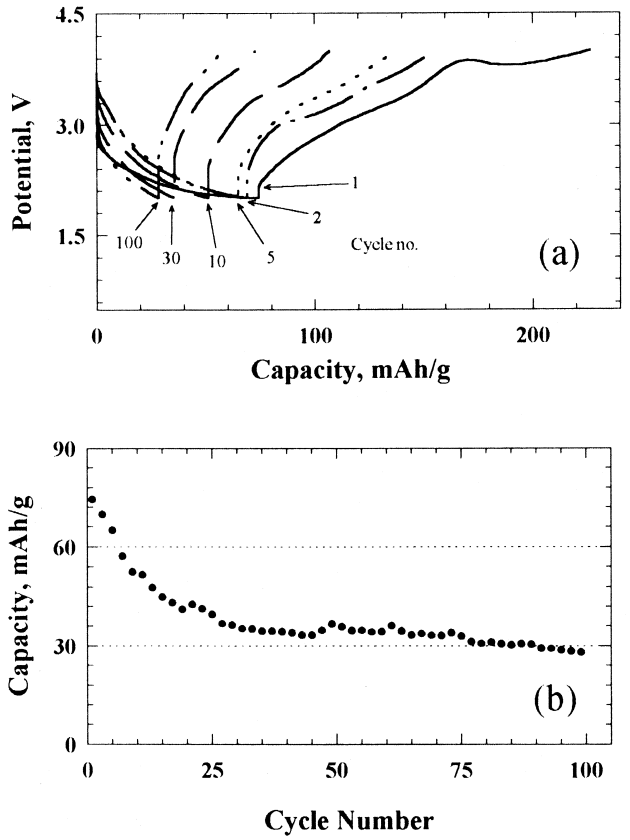

Fig. 8. (a) Cycling curves and (b) capacities as a function of cycle number at 0.2 mA cm^{-2}.

Fig. 8 shows the cycling process and capacity as a function of cycle number for a current density of 0.2 mA cm^{-2}. The first cycle is irreversible. But, the following cycling processes become reversible. A loss in capacity occurs during cycling. This is due to dissolution of Fe^{2+} ions and structural deformation of the cathode electrode. The main problem is degradation of the adhesion between the cathode laminate and the current-collector during cycling [13]. If this problem can be solved, then it will be possible to develop a secondary Li/FeOOH(an) polymer battery.

4. Conclusions

The diffusion coefficient of Li^+ ions inside a FeOOH(an) cathode is determined by a current–pulse relaxation method and chronoamperometry and has respective values of 1.4×10^{-8} and 1.1×10^{-8} cm^2 s^{-1}. Using the a.c. impedance spectroscopy, the valve is 2.97×10^{-11} cm^2 s^{-1}. These values indicate that normal diffusion of Li^+ ions occurs inside the composite cathode. The investigated impedance parameters suggest that considerable changes in the SPE/FeOOH(an) interface occur by deformation of the FeOOH(an) composite cathode electrode. Dissolution of Fe^{2+} ions appears at the termination of the first charge. It is induced by a particular composition of the composite cathode. In other words, the amount of conductive material is small and the $LiClO_4$ salt is involved in the cathode as a component part of polymer binder.

Although the first cycle is irreversible, cycling processes become reversible from the second cycle onwards. The initial specific discharge capacity at 0.1 mA cm^{-2} (about 1/14 C) is 130 mA h g^{-1} ($x = 0.6$) in potential range 2.0 to 4.0 V.

References

[1] M.S. Whittingham, Prog. Solid State Chem. 12 (1978) 41.
[2] Z. Takehara, K. Kanamura, N. Imamishi, C. Zhen, Bull. Chem. Soc. Jpn. 62 (1989) 1567.
[3] K. Kanamura, C. Zhen, H. Sakaebe, Z. Takehara, J. Electrochem. Soc. 138 (1991) 331.
[4] H. Sakaebe, S. Higuchi, J. Electrochem. Soc. 142 (1995) 360.
[5] K. Kanamura, H. Sakaebe, H. Fujimoto, Z. Takehara, J. Electrochem. Soc. 142 (1995) 2126.
[6] K.M. Abraham, M. Alamgir, J. Electrochem. Soc. 137 (1990) 1657.
[7] B.V. Ratnakumar, G. Nagasubramanian, S.D. Stefano, C.P. Bankston, J. Electrochem. Soc. 139 (1992) 1513.
[8] R. Xue, H. Huang, M. Menetrier, L. Chen, J. Power Sources 43–44 (1993) 431.
[9] F. Croce, F. Gerace, G. Dautenzenberg, S. Passerini, G.B. Appetecchi, B. Scrosati, Electrochim. Acta 39 (1994) 2187.
[10] J. Bard, L.R. Faulkner, Electrochemical Methods; Fundamentals and Applications, Wiley, New York (1980).
[11] S.I. Pyun, J.S. Bae, Electrochim. Acta 41 (1996) 919.
[12] N. Bonanos, B.C.H. Steels, E.P. Butler, Impedance spectroscopy; Emphasizing Solid Materials and Systems, in: J.R. Macdonald (Ed.), Wiley, New York (1987) p. 227.
[13] M. Alamgir, K.M. Abraham, Lithium Battery; New Materials, Developments, and Perspectives, in: G. Pistoia (Ed.), Elsevier, Amsterdam (1994) p. 127.